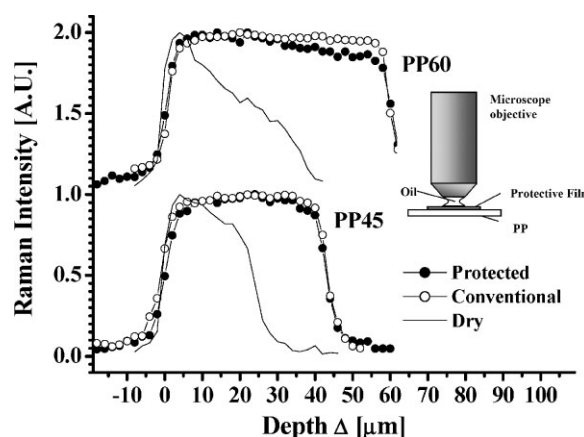


# Confocal Raman Microspectroscopy: A Non-Invasive Approach for in-Depth Analyses of Polymer Substrates

J. Pablo Tomba,\* José M. Pastor

We present a simple approach that avoids the problem of coupling fluid-sample interaction in confocal Raman depth-profiling with immersion objectives. We use a thin protective medium (PE film) that preserves the sample from direct contact with the coupling fluid, and that can be readily attached/de-attached from the sample surface by applying a small difference of pressure. The strategy was tested performing confocal Raman depth profiling studies on a series of transparent substrates (PP films; 25, 44 and 60  $\mu\text{m}$  nominal thickness) and comparing the results with those obtained with conventional approaches. It is shown that the strategy recovers very well all the film features, preserving at the same time a good depth resolution and optical throughput.



## Introduction

Confocal Raman microspectroscopy (CRM) is a powerful analytical tool that allows analysis of materials at sub-micron level with minimum sample preparation.<sup>[1,2]</sup> The confocal system restricts the sampled volume by placing an aperture at suitable points before the detector; this aperture blocks out-of-focus and off-axis scattered light thus improving both lateral and on-axis discrimination. Rich spectral information, sensitive to molecular, environmental and structural features, can thus be obtained from

confined sample regions located either over the sample surface or within the material.

Depth profiling is one of the probing modes of CRM. This approach, essentially non-destructive, is also referred to as *optical sectioning*, to stress differences with the conventional but destructive and invasive *mechanical sectioning*. In depth profiling, the sample is moved along the optical axis and a series of Raman spectra are acquired at different depths. Depth profiling is especially useful for studies of transparent materials and has naturally found many application niches in the polymer field, to study polymer laminates, distribution of species, crystals or inclusions in polymer matrices, among many others examples.<sup>[3–9]</sup>

The quantification of spatial discrimination in depth profiling studies, i.e. depth resolution, has been a major issue in CRM. In confocal microscopy, diffraction theory predicts that limiting values of depth resolution are proportional to laser wavelength ( $\lambda$ ) and to the inverse square of the numerical aperture (NA) of the microscope objective employed.<sup>[10]</sup> For a standard instrumental

J. P. Tomba

Institute of Materials Science and Technology (INTEMA), National Research Council (CONICET), University of Mar del Plata, Juan B. Justo 4302, (7600) Mar del Plata, Argentina

E-mail: jptomba@fi.mdp.edu.ar

J. M. Pastor

Department of Physics of Condensed Matter, University of Valladolid, Paseo del Cauce s/n, (47011) Valladolid, España

configuration ( $\lambda = 632\text{ nm}$ ,  $\text{NA} = 0.9$ ) depth resolution values below one micron are predicted. These predictions are only valid if there is no mismatch of refractive index ( $n$ ) between the medium through which the laser beam travels and the sample. If significant refractive index discontinuity exists refraction effects have to be considered. This is the case when dry metallurgical objectives, designed to operate through air, are employed for depth-profiling of transparent solid samples, for which  $n$  values typically found are larger than 1.4. Theory and experiments demonstrate that deviation of the laser beam at the sample entrance by refraction causes significant spreading of the laser focal volume with the consequent worsening in depth resolution, by one order of magnitude or more compared with the values predicted by diffraction theory.<sup>[11,12]</sup> This deterioration in depth resolution is not steady and becomes more severe as one focuses deeper below the sample surface. Another undesirable effect is that the depth scale is artificially compressed making sample features to appear artificially closer to the microscope objective. Laser refraction also perturbs the collection efficiency of the confocal aperture causing a continuous and dramatic reduction in detected intensity with focusing depth.<sup>[13–15]</sup>

An effective way to preserve depth resolution within the diffraction limits is the use of a coupling fluid that matches the refractive index of the sample analyzed.<sup>[16]</sup> In confocal fluorescence microspectroscopy, for instance, the use of water-immersed objectives in biological or medical applications is standard. In CRM, one may find several organic oils potentially available as coupling media that match well the range of  $n$  values typically found in polymers ( $n \approx 1.5$ ). Unfortunately, many polymeric substrates, particularly those amorphous, do not tolerate the direct contact with organic liquids: organic molecules can penetrate and swell the substrate by diffusion, cause extensive damage (i.e. cracking) by osmotic swelling or dissolve the polymer in case of thermodynamic affinity.

In this work, we present a strategy that tackles the problem of polymer-coupling fluid interaction in depth profiling by CRM with immersion objectives. The strategy is based on the use of a protective coating as a separating medium to avoid substrate-coupling fluid direct contact. A key point is that the coating can be reversibly attached/de-attached to/from the sample surface by applying a small difference of pressure. The approach is compared with conventional methods and its efficiency, in terms of sample protection and quality of data acquired, is evaluated.

## Experimental Part

The poly(propylene) (PP) and low density polyethylene (PE) films used here are commercially available. The coupling oil was

purchased from Merck (B446082). The PE film used as protective coating has a nominal thickness of  $30\text{ }\mu\text{m}$ . The PP films used as test samples were 25, 44 and  $60\text{ }\mu\text{m}$  thick and will be referred to as PP25, PP45 and PP60 hereafter. All film thicknesses were measured with a Mitutoyo micrometer (model 395-271), with  $\pm 1\text{ }\mu\text{m}$  precision. Refractive indexes of the components of the experimental setup were all close to 1.5: 1.51 (PE), 1.49 (PP) and 1.50 (coupling oil).

Non-polarized Raman spectra were recorded at room temperature, on a Raman microspectrometer (DILOR Confocal Laser Raman, LabRam), equipped with a 16-mW He-Ne laser beam ( $632.8\text{ nm}$  wavelength). A slit width of  $500\text{ }\mu\text{m}$  and a holographic grating of  $1800\text{ lines}\cdot\text{mm}^{-1}$  yielded a spectral resolution of about  $4\text{ cm}^{-1}$ . Micro measurements were carried out with an immersion Olympus  $100\times$  objective ( $\text{NA} = 1.3$ ,  $210\text{ }\mu\text{m}$  working distance). The confocal aperture was set to  $200\text{ }\mu\text{m}$ . The nominal depth resolution in these conditions was determined by scanning in  $z$ -direction the intensity of the  $520\text{ cm}^{-1}$  band of a silicon wafer immersed in the coupling oil.<sup>[17]</sup> Silicon acts as a layer of infinitesimal thickness, providing the point-by-point depth response of the instrument. The full width at half maximum of the bell shaped curve obtained was  $4.3\text{ }\mu\text{m}$  (see Figure 5 below).

The protecting PE coating was applied onto the surface of the test samples through a home-made device; more details can be found elsewhere.<sup>[18]</sup> The whole assembly and its main parts are shown in Figure 1. An aluminum frame, internally threaded, supports the protective coating. The film was cut from the original sheet to perfectly fit in the dimensions of the frame. The internal diameter of the frame,  $30\text{ mm}$ , allows the housing of the microscope objective ( $18\text{--}24\text{ mm}$  diameter). An externally threaded aluminum ring tightly fixes the edges of the protective film to the frame, maintaining the film in place. To promote good physical contact between these elements, we evacuated the air between them through a channel performed in the main frame, in turn connected to a standard laboratory vacuum pump. A rubber o-ring placed between frame and sample prevents air entrance helping to keep a low pressure at one of the sides of the coating.

For depth-profiling, the model sample, protected with the PE film on top through the above-described system, was directly

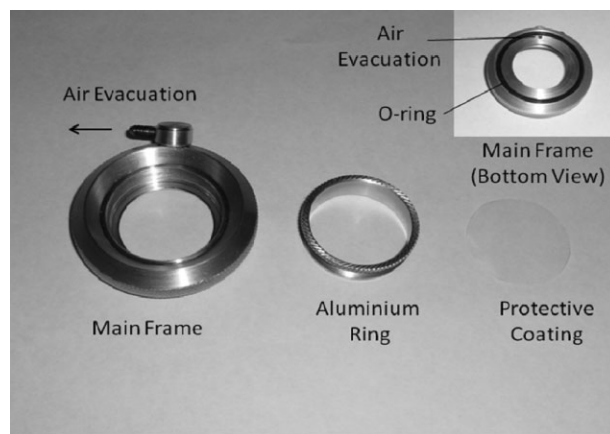


Figure 1. Main components of the experimental setup used to reversibly apply the protective film.

mounted on the microscope stage. Test PP samples were supported onto a glass slide. Good optical contact between PP and glass was achieved by placing a drop of coupling oil between them, as suggested in ref.<sup>[16]</sup> Air evacuation was sustained during measurements. A drop of coupling oil was applied onto the surface of the protective film, as in conventional depth profiling with immersion optics, to minimize deviations of the laser path at the sample entrance. Confocal depth profiles were obtained by moving the sample through the focus point, in steps of 2  $\mu\text{m}$ , via vertical displacement of the microscope stage (z-axis), controlled manually with the micrometric screw of the microscope with a 0.5  $\mu\text{m}$  precision.

## Results and Discussion

### Spectral Properties and in-Depth Profiles Construction

The characteristic Raman spectra of the components of the experimental setup, i.e., coupling oil, protective coating and substrate, are shown in Figure 2, for the range of Raman shifts 720–1 640  $\text{cm}^{-1}$ . The spectral profiles are markedly different, which allows easy differentiation between components. To follow in-depth individual distribution, we tracked variations in Raman intensity of specific bands as a function of focusing depth. We have chosen the band at  $\approx 1\,000\text{ cm}^{-1}$  as characteristic for the coupling oil, that at  $\approx 1\,295\text{ cm}^{-1}$  for the protective coating (PE) and the band at  $806\text{ cm}^{-1}$  for the PP substrate. We see that this assignation is almost free of spectral overlapping allowing safe quantification of component distributions. To construct confocal Raman in-depth profiles, we plotted individual band intensities, as obtained from the raw local spectrum, as a function of focusing depth, as determined from the micrometric screw of the microscope stage. No corrections

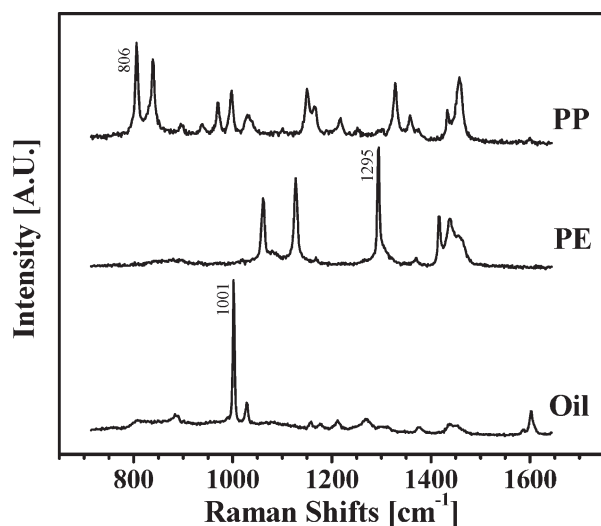


Figure 2. Raman spectra of individual components.

on the depth scale were made. In earlier treatments of the topic, it has been common to refer to this variable as  $\Delta$ , the nominal focusing depth; we will follow this notation throughout the work.

### Test on Model Samples

We tested the proposed strategy by measuring the confocal in-depth Raman response of a series of model PP substrates with well characterized thickness, supported onto a glass slide. In these experiments, we protected the PP samples with the PE coating, as detailed in the experimental part. Despite of the presence of a crystalline phase, PE is relatively transparent to the visible 632 nm laser used as excitation source. A key point for the success of the strategy is to obtain a uniform optical path for the laser beam when passing from coating to substrate, which is achieved in this case by air evacuation between elements. Once air is evacuated by the pump, the difference of pressure thus established at both sides of the protective film is largely enough to tightly adhere it to the counterpart. At the same time, the PE film is flexible enough to copy possible surface imperfections of the substrate, helping to achieve good physical contact with most parts of the sample surface. This quality has been another reason for choosing a low density PE as material for the protective coating: it has good mechanical integrity but nice flexibility due to its relatively low crystalline content. At the same time, and due to the semicrystalline nature of the polymer, it resists relatively well the contact with organic species. In any case, the coating can be easily replaced between measurements if it presented signs of damage. We also tried with other semicrystalline transparent films commercially available, i.e. polyethylene terephthalate or PP, but they were too stiff for this application.

Figure 3 shows as-measured confocal profiles for one of the model systems (PP25). The zero in the depth scale

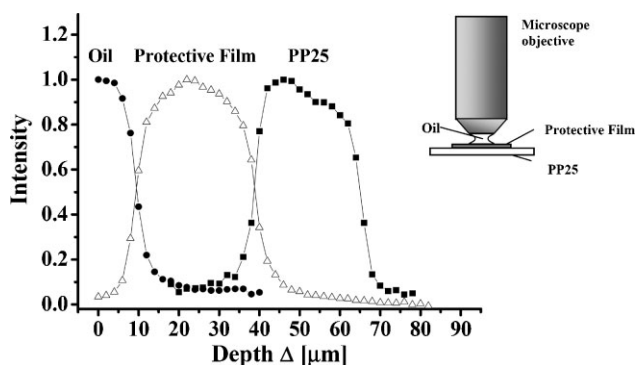
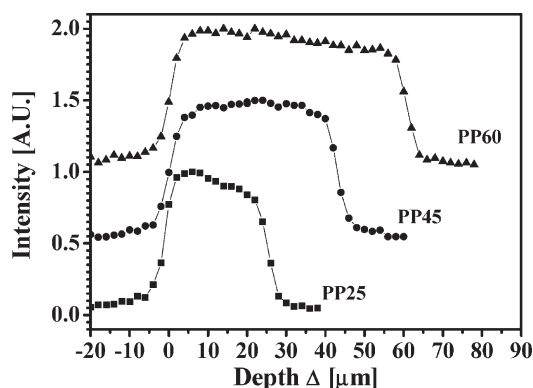


Figure 3. Confocal profiles of the test system (PP25), showing the in-depth distribution of the other components (PE, oil). The profiles have been normalized to unity.

( $\Delta$ , nominal focusing depth) corresponds to some arbitrary point within the coupling oil layer where depth-profiling was originally started. In the  $y$ -axis we plotted the intensity of the Raman bands specific to each component, normalized with respect to its maximum value. The oil used as coupling fluid appears here in the 0–10  $\mu\text{m}$  depth range, followed by the response of the protective coating, which extends from 9.5 to 39  $\mu\text{m}$ , as determined from the full-width at half-maximum (FWHM) of the profile. The apparent thickness of the PE coating is about 29.5  $\mu\text{m}$ , in good agreement with the expected value (30  $\mu\text{m}$ ); this is not surprising giving the good optical contact between the coupling oil, a viscous liquid, and the PE film, having both similar refractive indexes. The response of the PP25 test film is found at higher depths (39–65  $\mu\text{m}$ ); its apparent thickness (26  $\mu\text{m}$ ) is almost identical to the nominal value (25  $\mu\text{m}$ ). This good agreement indicates that the depth scale is not artificially compressed as in cases where refraction dominates.<sup>[11,12,17]</sup>

Figure 4 shows the confocal response of the whole set of test PP films analyzed. The confocal profiles have been shifted horizontally with respect to the maximum of the derivative curve of the respective intensity profile and vertically by 0.5 units (PP45) and by 1.0 unit (PP60), to facilitate visualization. The zero in the depth scale corresponds now to the coating/substrate interface. We see that the strategy recovers very well the main features of the PP films. The apparent film thickness is in all cases close to the expected values, obtained from independent measurements. The shape of the confocal responses is visually similar to the boxcar functions one would expect as the true free-of-artifacts film response. The intensity throughout the film is quite constant, in contrast with the marked intensity decrease with nominal depth typically reported in depth profiling with dry objectives, see Figure 6 below. We also see that the broadening of all the planar interfaces found (oil-PE, PE-PP, PP-glass) is rather similar



**Figure 4.** Confocal profiles of the PP films as determined with the proposed strategy. Profiles have been vertically and horizontally offset for clarity. The zero in the depth scale corresponds to the coating/substrate interface.

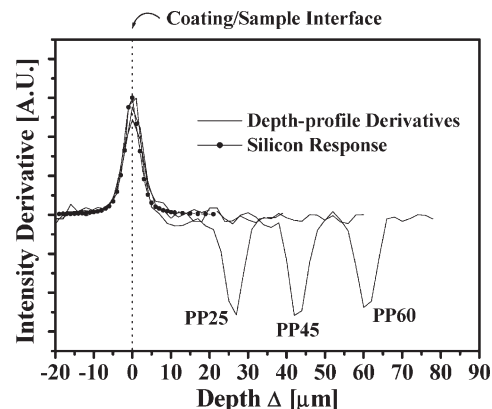


**Figure 5.** Derivatives of the PP confocal profiles shown in Figure 4. Superimposed, we show the depth-response of Silicon, obtained by depth-profiling the 520  $\text{cm}^{-1}$  Raman band.

indicating that depth resolution does not degrade substantially with focusing depth.

A finer analysis in terms of actual instrumental response can be performed through the derivative curves of the PP confocal profiles, as shown in Figure 5. Derivatives have been shifted horizontally with respect to their maxima. While the derivative maximum reveals the position of the coating/substrate interface, the derivative minimum indicates the apparent film thickness: the values obtained from the plot (27, 42 and 60  $\mu\text{m}$ ) are in excellent agreement with nominal thickness of the PP substrates (25, 44 and 60  $\mu\text{m}$ ).

The width of the peaks of the first derivative profile provides a measure of the actual depth resolution assuming that the true PP intensity distributions can be represented as boxcar functions limited by the PE/PP and PP/glass interfaces, and that the thickness of the PP films are much greater than depth resolution; both conditions

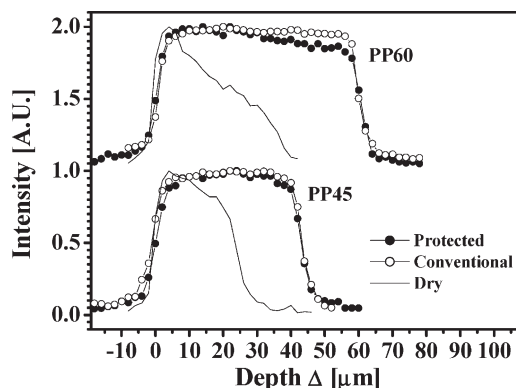


**Figure 6.** Comparison of the confocal response of PP films, as measured through the protective film and in conventional way. In both cases, the objective was an oil immersion Olympus 100 $\times$  (NA = 1.3), in conjunction with a confocal aperture of 200  $\mu\text{m}$  and a coupling oil with  $n = 1.5$ . Dry measurements were carried out with an Olympus 100 $\times$  (NA = 0.9).



hold in our case. We see that the peak width of all the planar interfaces found (PE-PP, PP-glass) is rather similar, confirming that depth resolution remains fairly constant with focusing depth. Also important, operative depth resolution is comparable to that obtained from depth-scanning of silicon. To stress this point we have included in the plot the intensity response of the silicon wafer, which provides the point-by-point depth response of the instrument in absence of refraction; for details on how this function was obtained see the Experimental Part. The function has been shifted horizontally and vertically rescaled, to facilitate the comparison. We see that the derivative responses of all PE/PP interfaces can be well superimposed with the silicon response, and that they are also comparable to those of the PP/glass interfaces. This good matching confirms that the strategy preserves very well the nominal depth resolution in the range of depths analyzed.

### Comparison with Conventional Approaches

To complete the analysis, we directly compare our results with those obtained with conventional methods, i.e. immersion objectives with the coupling oil directly applied onto the PP film. We have also included results obtained with dry objectives, i.e. PP films directly profiled through air, without coupling fluid. Figure 6 shows this type of data for two of the films studied (PP45 and PP60). In the comparison, the PP responses have been shifted with respect to the maximum of the derivative curve of the respective intensity profile and have been scaled with respect to unity. The open symbols correspond to PP responses obtained with conventional depth-profiling with immersion optics, while the solid symbols shown data acquired with the approach presented here. We see that both strategies yielded practically the same confocal response. In terms of intensity of collected Raman signal, we observed a minor decrease, about 10%, with respect to the conventional approach. This intensity loss is likely due to the presence of crystals in the PE protective coating, which scatter light decreasing transparency.<sup>[17,19]</sup> The response measured with a dry 100 $\times$  objective (NA = 0.9), represented with solid lines, underestimates the film thickness by a factor of  $\approx 1.7$  and drops continuously throughout the film. Both features, typical of dry depth-profiling, have been extensively documented in the literature and illustrate the convenience of the use of immersion optics to carry out safe and precise in-depth studies.

### Other Approaches for Non-Invasive Depth-Profiling

We end the paper with a brief summary of strategies other than that developed here that can be adapted for non-invasive depth-profiling. On the experimental side, Vyorka et al.

implemented the use of a double oil configuration, with a thin glass as a separating element between different oils.<sup>[20]</sup> This approach utilizes an oil-immersion objective, compatible with one of the fluids, and a second fluid in contact with the sample. The user has in this case more freedom to choose the second fluid to properly minimize sample interaction, spectral overlapping or discontinuities in refractive index. Overall, as long as fluids and separating media have similar refractive indexes, the approach is expected to keep all the benefits of immersion techniques: steady depth resolution and good intensity throughput. Adar et al. tested the use of microscope objectives with cover slip correction, i.e. a dry objective corrected to be used through a cover glass or window of a given thickness.<sup>[21]</sup> The approach is proposed to study inclusions below the surface of a polymeric matrix, where the objective is expected to correct for the presence of the matrix layer between objective and inclusion. It was shown that the approach yields higher intensity of Raman scattering compared with traditional uncorrected dry objectives. Later work has shown that other features, such as the artificial compression on the depth scale or the degradation in depth resolution with focusing depth, are not avoided when substrates with refractive index higher than 1 are profiled, limiting in part the usefulness of the original proposal.<sup>[16]</sup>

The results shown here have encouraged us to investigate other alternatives, based on the use of viscous liquids with controlled flow, instead of the solid protective coating and the coupling oil used in the present configuration. For instance, we are currently exploring the use of polymers with low glass transition temperature ( $T_g$ ), lightly cross-linked, which can be directly used instead of the coupling oil. At room temperature, a low  $T_g$  polymer behaves as a highly viscous fluid, able to fill well the space between sample and objective and to produce a good conformal contact with the sample; at the same time cross-linking should limit the ability of the polymer to flow and to penetrate in the sample under study by diffusion. Polymers based on poly(dimethyl siloxane) ( $n \approx 1.5$ ) are being evaluated as candidates for this use; one of the reasons is its perfect transparency due to the lack of crystals. PE copolymers with very low crystal content are also being considered; in this case the ability to flow is limited by the presence of crystals.

On the numerical side, we find several mathematical treatments that predict, with different levels of rigor and sophistication, the combined effects of laser refraction and diffraction on depth resolution.<sup>[14,17,22,23]</sup> We could use these models as a tool to correct raw data obtained with dry objectives, such as those shown in Figure 6, avoiding the use of oils. These approaches have shown to be useful to directly correct the apparent compression on the depth scale, through a rescaling factor.<sup>[17,23,24]</sup> The successive enlargement of the sampled region with focusing depth is

also well predicted,<sup>[17,22]</sup> however, this correction has only been applied in direct way, i.e. by convolution of a pre-established intensity function with the instrumental depth response<sup>[17,25]</sup> that can then be compared with the experiment. Mathematical schemes aimed at solving the inverse problem for this specific case, i.e. to obtain corrected data from the raw experiment by deconvolution, have only been developed for some specific cases;<sup>[26]</sup> there is however a lack of a more generalized and reliable approach to apply. Nevertheless, none of these numerical corrections can avoid the dramatic drop in overall Raman intensity with nominal focusing depth that penalizes the quality of the spectral data one obtains at large depth values.

## Conclusion

We have shown an approach that circumvents the problem of coupling fluid-polymeric substrate interaction in depth profiling with immersion optics, through the use of a coating that avoids direct contact between these elements. The implementation of the approach is rather simple and does not require particular sample preparation. There are some obvious limitations in terms of specimen dimensions and surface roughness of the sample, but they are not much more stringent than those required for carrying out conventional depth profiling with immersion objectives. The fact that the refractive index of the protective coating cannot be finely tuned, as in the case of organic oils, does not appear as a serious limitation as most of the polymer samples susceptible to be depth-profiled have  $n$  values in ranges very close to 1.5. Overall, we have shown that with this approach, it is possible to carry out genuine optical sectioning of polymeric substrates with invariant depth-resolution, close to the diffraction limit, and good optical throughput.

**Acknowledgements:** This work is part of a project funded by ANPCYT (PICT06-1359) and AECID (A60606).

Received: November 26, 2008; Revised: January 21, 2009;  
Accepted: January 23, 2009; DOI: 10.1002/macp.200800582

**Keywords:** films; raman spectroscopy; refractive index

- [1] G. J. Puppels, F. F. M. de Mul, C. Otto, J. Greve, M. Robert-Nicoud, D. J. Arndt-Jovin, T. M. Jovin, *Nature* **1990**, *347*, 301.
- [2] G. P. Puppels, W. Colier, J. H. F. Olminkhof, C. Otto, F. F. M. de Mul, J. Greeve, *J. Raman Spectrosc.* **1991**, *22*, 217.
- [3] J. P. Tomba, L. Arzondo, J. M. Carella, J. M. Pastor, *Macromol. Chem. Phys.* **2007**, *208*, 1110.
- [4] L. Arzondo, J. P. Tomba, J. M. Carella, J. M. Pastor, *Macromol. Rapid Commun.* **2005**, *26*, 632.
- [5] O. S. Fleming, F. Stepanek, S. G. Kazarian, *Macromol. Chem. Phys.* **2005**, *206*, 1077.
- [6] B. Marton, L. G. J. van der Ven, C. Otto, N. Uzunbajakava, M. A. Hempenius, G. J. Vansco, *Polymer* **2005**, *46*, 11330.
- [7] F. Belaroui, Y. Grohens, H. Boyer, Y. Holl, *Polymer* **2000**, *41*, 7645.
- [8] J. Sacristan, H. Reinecke, C. Mijangos, S. Spells, J. Yarwood, *Macromol. Chem. Phys.* **2002**, *203*, 678.
- [9] J. Sacristan, C. Mijangos, H. Reinecke, S. J. Spells, J. Yarwood, *Macromol. Rapid Commun.* **2000**, *21*, 894.
- [10] C. B. Juang, L. Finzi, C. J. Bustamante, *Rev. Sci. Instrum.* **1988**, *59*, 2399.
- [11] N. Everall, *Appl. Spectrosc.* **2000**, *54*, 773.
- [12] N. Everall, *Appl. Spectrosc.* **2000**, *54*, 1515.
- [13] K. J. Baldwin, D. N. Batchelder, *Appl. Spectrosc.* **2001**, *55*, 517.
- [14] J. L. Bruneel, J. C. Lassegues, C. Sourisseau, *J. Raman Spectrosc.* **2002**, *33*, 815.
- [15] J. P. Tomba, J. M. Pastor, *Vib. Spectrosc.* **2007**, *44*, 62.
- [16] N. Everall, J. Lapham, F. Adar, A. Whitley, E. Lee, S. Mamedov, *Appl. Spectrosc.* **2007**, *61*, 251.
- [17] J. P. Tomba, L. M. Arzondo, J. M. Pastor, *Appl. Spectrosc.* **2007**, *61*, 177.
- [18] J. P. Tomba, J. M. Pastor, *Appl. Spectrosc.* **2008**, *62*, 817.
- [19] A. M. Macdonald, A. S. Vaughan, *J. Raman Spectrosc.* **2007**, *38*, 584.
- [20] J. Vyorykka, J. Halttunen, H. Iitti, J. Tenhunen, T. Vuorinen, P. Stenius, *Appl. Spectrosc.* **2002**, *56*, 776.
- [21] F. Adar, C. Naudin, A. Whitley, R. Bodnar, *Appl. Spectrosc.* **2004**, *58*, 1136.
- [22] C. Sourisseau, P. Maraval, *Appl. Spectrosc.* **2003**, *57*, 1324.
- [23] S. J. Spells, H. Reinecke, J. Sacristan, J. Yarwood, C. Mijangos, *Macromol. Symp.* **2003**, *203*, 147.
- [24] H. Reinecke, S. J. Spells, J. Sacristan, J. Yarwood, C. Mijangos, *Appl. Spectrosc.* **2001**, *55*, 1660.
- [25] J. Vyorykka, J. Paaso, M. Tenhunen, J. Tenhunen, H. Iitti, T. Vuorinen, P. Stenius, *Appl. Spectrosc.* **2003**, *57*, 1123.
- [26] A. Gallardo, S. Spells, R. Navarro, H. Reinecke, *Macromol. Rapid Commun.* **2006**, *27*, 529.